Applied Catalysis B: Environmental 329 (2023) 122552

Contents lists available at ScienceDirect

Applied Catalysis B: Environmental

journal homepage: www.elsevier.com/locate/apcatb

Facile one-pot synthesis of Fe-UZM-35 catalysts for ammonia selective catalytic reduction

Xuechao Tan [1], Shoute Zhang [1], Suk Bong Hong [*]

Center for Ordered Nanoporous Materials Synthesis, Division of Environmental Science and Engineering, POSTECH, Pohang 37673, South Korea

ARTICLE INFO

Keywords:
UZM-35 and Fe-UZM-35
Interzeolite conversion route
One-pot synthesis
High reproducibility
NH_3-SCR

ABSTRACT

Owing to the narrow crystallization field, the synthesis of the large-pore zeolite UZM-35 with MSE topology starting from amorphous reagents in the presence of dimethyldipropylammonium ions as an organic structure-directing agent is often non-reproducible. Here we report the synthesis of UZM-35 via an interzeolite conversion route using USY zeolites, as the sole source of Al and Si, and a small amount of previously synthesized UZM-35 as seed crystals. We also present the one-pot synthesis of Fe-UZM-35 with the best low-temperature NH_3-SCR activity among the iron-exchanged zeolites reported so far. These synthesis routes showed high reproducibility, together with considerably faster crystallization kinetics (≤1.5 vs 7 days) compared to conventional UZM-35 synthesis. When the Fe loading level was properly adjusted, the NH_3-SCR activity of one-pot-synthesized Fe-UZM-35 was found to be essentially the same as that of post-synthetically exchanged Fe-UZM-35 due to the similarity in the nature of their iron active sites.

1. Introduction

Despite an ambitious global market ramp-up of battery-electric passenger vehicles over the past decade, it is likely that diesel vehicles with high NO_x (NO and NO_2) emissions will not be completely phased out from our daily lives in the near future. In fact, diesel heavy-duty vehicles are predicted to remain a major freight transportation sector and should not be replaced by electric ones even in California at least until 2040, not only because of the economic reason but also because of the overall emission control strategy [1]. This becomes clearer when considering common rail systems, long-distance ships, and heavy construction and agriculture equipment, which currently use diesel engines, but might be difficult to be ubiquitously electrified before long.

Among the diesel exhaust after-treatment technologies developed so far, selective catalytic reduction of NO_x by NH_3 (NH_3-SCR) is most successful, but presents many challenges [2–4]. For example, the current commercial copper-exchanged SZZ-13 (framework type CHA) and SSZ-39 (AEI) catalysts [5,6] have poor resistance to poisoning from residual sulfur in diesel exhaust and favor the formation of N_2O, another potent greenhouse gas [7], during NH_3-SCR. In contrast, the other commercial NH_3-SCR catalysts, iron-exchanged beta and ZSM-5 (MFI) zeolites, with high resistance to sulfur poisoning and N_2O formation [8,9], suffer from poor low-temperature (<350 °C) SCR activity. In this respect, Fe-UZM-35 (MSE) with intersecting 12- and 10-ring channels is of special interest, because its low-temperature activity is best among the Fe-zeolites known to date [10,11]. Owing to its lower oxidation state, on the other hand, the Fe^{2+} ion can be more favorably exchanged into the aluminosilicate zeolite support than the Fe^{3+} ion. However, Fe^{2+} exchange in zeolites requires the prevention of Fe^{2+} oxidation to trivalent iron species such as FeO(OH), which cannot be easily introduced into the zeolite pores during ion exchange [9,12], requiring the use of inert N_2 atmosphere. One way to overcome such a limitation is the one-pot synthesis of Fe-zeolites (Fig. 1). Compared to Cu-zeolites, nevertheless, less attention to their one-pot synthesis has been paid so far [13–20]. To our knowledge, in particular, no attempt to one-pot-synthesize Fe-UZM-35 have been made yet.

We have previously shown that the Si/Al and $K^+/(Na^+ + K^+)$ ratios in the synthesis mixture yielding pure UZM-35 in the presence of dimethyldipropylammonium (DMDPA) ions as an organic structure-directing agent (OSDA) is very narrow [21]. Furthermore, the phase purity of this large-pore zeolite was found to be highly sensitive to crystallization time, giving limited reproducibility to its conventional hydrothermal synthesis starting from amorphous reagents. The interzeolite conversion (IZC) route, pioneered by Zones in the late 1980s

* Corresponding author.
E-mail address: sbhong@postech.ac.kr (S.B. Hong).
[1] These authors contributed equally to this work.

https://doi.org/10.1016/j.apcatb.2023.122552
Received 25 January 2023; Received in revised form 24 February 2023; Accepted 28 February 2023
Available online 2 March 2023

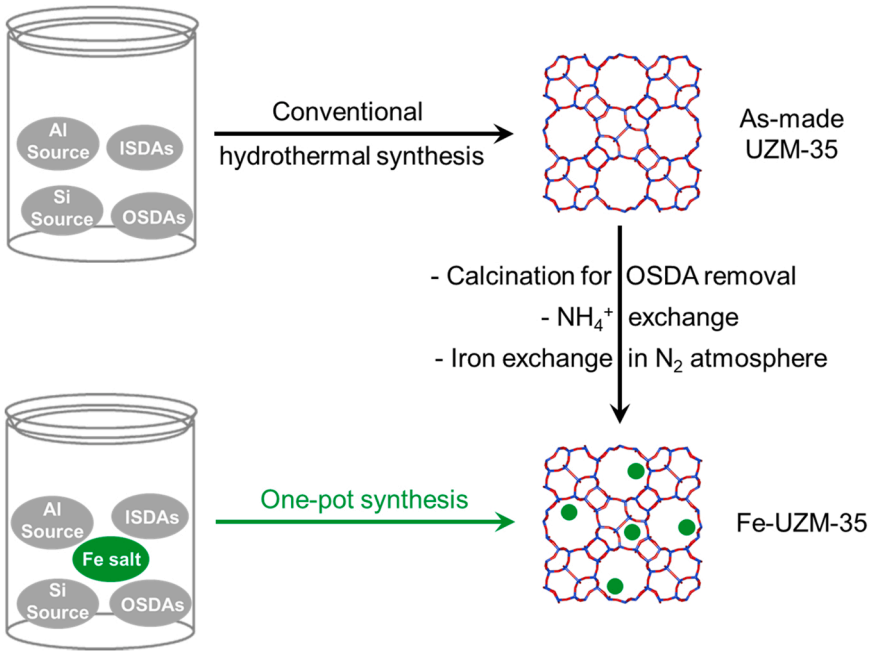

Fig. 1. Schematic illustrations of conventional and one-pot synthesis routes to Fe-UZM-35.

[22–24], includes the use of a particular zeolite as the source of Al, Si, and/or both, most likely zeolite Y (FAU), in the presence or absence of OSDAs. While the number of zeolite structures which can be synthesized through IZC is steadily growing [25], the reproducibility of zeolite synthesis is often method-specific. This has led us to consider whether the IZC route is applicable to the synthesis of UZM-35. Here we show that while the IZC of ultra-stable Y (USY; FAU) zeolites with DMDPA is a highly reproducible route to UZM-35, the one-pot synthesis of Fe-UZM-35 can also be achieved in a similar manner. The overall NH_3-SCR activity of one-pot-synthesized Fe-UZM-35 with an Fe/Al ratio of 0.23 (2.3 Fe wt%) was found to be comparable with that of post-synthetically exchanged Fe-UZM-35 with essentially the same Fe/Al ratio (0.24).

2. Experimental

2.1. Zeolite synthesis

The reagents used in this study included DMDPAOH (40%, Sachem), NaOH (50% aqueous solution, Aldrich), KOH (45% aqueous solution, Aldrich), aluminum hydroxide ($Al(OH)_3{\cdot}1.0\ H_2O$, Aldrich), colloidal silica (Ludox HS-40, Dupont), three USY zeolites with Si/Al ratios of 7.5 (HSZ-360-HUA, Tosoh), 15 (CBV720, Zeolyst), and 30 (CBV760, Zeolyst), $FeSO_4{\cdot}7\ H_2O$ (99%, Aldrich), $CuSO_4{\cdot}5\ H_2O$ (98%, Aldrich), and NH_4NO_3 (98.5%, Alfa).

The conventional hydrothermal synthesis of UZM-35, which uses Al $(OH)_3{\cdot}1.0\ H_2O$ and Ludox HS-40 as Al and Si sources, respectively, was carried out according to the procedures given elsewhere [21]. Its IZC synthesis that uses USY as the sole source of Al and Si, as well as the one-pot synthesis of Fe-UZM-35, was performed using aluminosilicate gels with the composition $4.50DMDPAOH{\cdot}0.25Na_2O{\cdot}0.75\ K_2O{\cdot}x Fe^{II}O{\cdot}yAl_2O_3{\cdot}10.0SiO_2{\cdot}155\ H_2O$, where x and y are varied between $0 \leq x \leq 0.50$ and $0.017 \leq y \leq 0.067$, respectively. If required, a small amount of previously synthesized and calcined UZM-35 (4 wt% of USY used) was added as seed crystals. The one-pot synthesis of Cu-UZM-35 was also attempted in a similar manner to that of Fe-UZM-35. After being stirred for 2 h at a room temperature, the final mixture was placed into a 45 mL Teflon-lined autoclave and heated under static conditions at 170 °C for 0.5–7 days. The solid products were recovered by centrifugation, washed repeatedly with deionized water, and dried overnight at room temperature. As-made Fe-UZM-35 and Cu-UZM-35 were refluxed twice in 1.0 M NH_4NO_3 solutions (1 g solid per 100 mL solution) for 6 h and then calcined in air at 550 °C for 8 h, prior to their use as catalysts for NH_3-SCR.

Fe-UZM-35 and Cu-UZM-35 were also prepared by iron exchange of the ammonium form of UZM-35 synthesized by the conventional method, following the procedures described in our previous work [10,11,21]. All catalysts prepared here were hydrothermal aged at 750 °C in air for 12 h, using flowing air consisting of 10% H_2O. While the UZM-35 zeolites synthesized via conventional and IZC synthesis routes were referred to as UZM-35(C) and UZM-35(IZC), respectively, the Fe-UZM-35 zeolites obtained by iron exchange of NH_4-UZM-35(C) and one-pot synthesis were denoted as Fe-UZM-35(C) and Fe-UZM-35(OP), respectively. When necessary, in addition, their Fe/Al ratio was attached to the catalyst name. For comparison, Fe-beta with Fe/Al = 0.21 was prepared by iron exchange of NH_4-beta with Si/Al = 12.5 (CBV814E, Zeolyst) and designated in a manner similar to that given above.

2.2. Catalysis

NH_3-SCR was performed in a continuous fixed-bed flow reactor. Before each catalytic run, 0.6 g of catalyst (20/30 mesh) was packed into a 3/8-in.-od aluminum tube reactor and pretreated at 500 ℃ for 2 h under air flow (2000 mL min^{-1}). A reactant feed containing NO 500 ppm, NH_3 500 ppm, 5% O_2, and 10% H_2O, balanced with N_2, was supplied, and the steady-state SCR conversion was measured at temperature ranging from 150° to 600°C at a gas hourly space velocity (GHSV) of 100,000 h^{-1}. The inlet and outlet gas concentrations were analyzed online by a Thermo Nicolet 6700 FT-IR spectrometer. The apparent activation energy (E_{app}) was determined from the slope of the Arrhenius plot according to the procedures given in our recent work [11].

2.3. Characterization

Powder X-ray diffraction (PXRD) patterns were collected on a PANalytical X'Pert diffractometer with Cu Kα radiation (λ = 1.5406 Å). The crystallinity of a series of solid products isolated as a function of

Table 1
Representative synthesis conditions[a] and results.

Run no.	Al source[b]	Si source[b]	Synthesis mixture composition[a]			Product[c]
			x	Si/Al	Fe/Al	
1[d]	AH	LH	0	10		UZM-35
2[d]	HSZ-360-HUA		0	7.5		Amorphous
3[e]	HSZ-360-HUA		0	7.5		Offretite + UZM-35
4	CBV720		0	15		Amorphous + (UZM-35)
5[e]	CBV720		0	15		UZM-35
6	CBV760		0	30		Amorphous + (UZM-35)
7[e]	CBV760		0	30		UZM-35
8[e]	CBV760		0.06	30	3.8	Fe-UZM-35
9[e]	CBV760		0.13	30	7.5	Fe-UZM-35
10[e]	CBV760		0.25	30	15	Fe-UZM-35
11[e]	CBV760		0.50	30	30	Amorphous + Fe-UZM-35
12[e,f]	CBV760		0.06	30	3.8[g]	Cu-UZM-35
13[e,f]	CBV760		0.08	30	5.0[g]	Cu-UZM-35
14[e,f]	CBV760		0.13	30	7.5[g]	Cu-UZM-35 + amorphous + (Cu-offretite)

[a] The synthesis mixture composition is 4.50DMDPAOH·0.25Na_2O·0.75 K_2O·$x$$Fe^{II}O$·$y$$Al_2O_3$·10.0$SiO_2$·155 H_2O, where x and y are varied between $0 \leq x \leq 0.50$ and $0.017 \leq y \leq 0.067$, respectively. All syntheses were conducted under static conditions at 170 °C for 4 days, unless otherwise stated.

[b] AH, $Al(OH)_3$·1.0 H_2O; LH, Ludox HS-40; HSZ-360-HUA, Tosoh USY with Si/Al = 7.5; CBV720, Zeolyst USY with Si/Al = 15; CBV760, Zeolyst USY with Si/Al = 30.

[c] The product appearing first is the major phase, and the product obtained in a trace amount is given in parentheses.

[d] Obtained after 7 days of heating at 170 °C.

[e] A small amount of calcined UZM-35(C) (4 wt% of USY used as both Si and Al sources) were added as seed crystals.

[f] $CuSO_4$·5H_2O was added instead of $FeSO_4$·7H_2O.

[g] Cu/Al ratio.

crystallization time during the synthesis of UZM-35(IZC) and Fe-UZM-35(OP) under static conditions at 170 °C was determined by comparing the area of the X-ray peak around $2\theta = 21.7°$, corresponding to the (420) reflection of the MSE structure, with that of as-made UZM-35(C) [26]. The crystallinity of the USY source during their crystallization was estimated by comparing the area of the intense X-ray peak around $2\theta = 6.2°$ assigned to the (111) reflection of the FAU structure with that of CBV760 USY. Crystal morphology and size were identified by a JEOL JSM-6510 scanning electron microscope (SEM). Thermogravimetric analysis (TGA) was conducted on a SII EXSTAR 6000 thermal analyzer, and the weight loss due to the combustion of OSDAs were determined from differential thermal analysis (DTA) using the same analyzer. Elemental analysis was carried out by the Pohang Institute of Metal Industry Advancement. The N_2 adsorption data were obtained on a Mirae SI nanoPorosity-XG analyzer.

^{27}Al MAS NMR spectra were measured on a Bruker DRX500 spectrometer at a ^{27}Al frequency of 130.351 MHz with a π/6 rad pulse length 1.0 μs, a recycle delay of 2.0 s, and an acquisition of ca. 1000 pulse transients. To accurately compare the signal intensity of fresh and hydrothermally aged catalysts, the same amount of sample was used in each experiment. IR spectra in the OH region were taken on a Thermo-Nicolet 6700 FT-IR spectrometer using self-supporting catalyst wafers of ca. 13 mg. Prior to the experiments, the wafer was treated under vacuum (10^{-4} Pa) at 450 °C for 2 h inside a home-built IR cell with CaF_2 windows. In situ diffuse reflectance infrared Fourier-transform (DRIFT) spectra were collected on an identical FT-IR spectrometer but with a DRIFT cell (Pike). Before each experiment, about 15 mg of catalyst was heated under air flow (100 mL min^{-1}) at 350 °C for 2 h. After being cooled down to 150 °C, a background spectrum was obtained. Then, the catalyst was exposed to 500 ppm NO with 5% O_2 in He for 1 h and then purged in a He flow at the same temperature for another 0.5 h. The spectra were measured and analyzed after subtracting the background.

Table 2
Physical properties of the representative catalysts studied in this work.

Run no.[a]	Catalyst ID	Si/Al[b]	Fe wt %[b]	Fe/Al[b]	Crystal shape and average size[c] (μm)	BET surface area[d] (m^2 g^{-1})
1	UZM-35 (C)	9			Rectangular plates, 0.3 × 0.15	420 (0.18)
5	UZM-35 (IZC)A	7				460 (0.19)
7	UZM-35 (IZC)B	8			Rectangular plates, 3.0 × 1.0	450 (0.19)
8	Fe-UZM-35(OP) 0.13	8	1.3	0.13		440 (0.19)
9	Fe-UZM-35(OP) 0.23	8	2.3	0.23	Rectangular plates, 1.5 × 1.5	440 (0.19)
10	Fe-UZM-35(OP) 0.38	8	3.7	0.38		440 (0.19)
13	Cu-UZM-35(OP) 0.11	7	1.3[e]	0.11[f]	Rectangular plates, 1.5 × 1.5	430 (0.19)

[a] The same as those in Table 1.

[b] Determined by elemental analysis.

[c] Determined by SEM.

[d] Determined by N_2 adsorption data of their proton form. The values in parentheses are the micropore volumes in cm^3 g^{-1}.

[e] Cu wt%.

[f] Cu/Al ratio.

UV-Vis spectra were taken on a Shimadzu UV-2501PC spectrometer using $BaSO_4$ as a reference.

X-band EPR spectra at − 148 °C were measured on a Bruker A200 spectrometer with 100 kHz field modulation and 41 s sweep time. The packing height of powdered sample in the tube was kept constant, with its center placed in the middle of the EPR cavity, in order to quantitatively measure the signal intensity. The g value was calibrated with 2,2-diphenyl-1-picrylhydrazyl powder (g = 2.0036). NH_3 temperature-programmed desorption (TPD) was collected on a Hewlett-Packard5890 series II gas chromatograph with a thermal conductivity detector, as described in our previous paper [27]. The X-ray absorption near edge structure (XANES) spectra at the Cu K-edge were recorded on the 8 C beamline at the Pohang Accelerator Laboratory using a Si (111) crystal monochromator, and further details can be found elsewhere [21].

3. Results and discussion

3.1. One-pot synthesis of Fe-UZM-35

Table 1 lists the summary of the IZC synthesis of UZM-35 under static conditions at 170 °C. The products listed in each synthesis run were the only ones found in repeated trials. Our initial attempt to obtain UZM-35 through IZC, with DMPDA as an OSDA, was by replacement of silica in the reported gel composition 4.50DMDPAOH·0.25Na_2O·0.75 K_2O·0.5Al_2O_3·10.0SiO_2·150 H_2O [21] with the equimolar amount of a Tosoh USY (Si/Al = 7.5, HSZ-360-HUA), without adding any Al source. However, the synthesis mixture remained an amorphous phase even after heating at 170 °C for 7 days. This led us to change the USY source to USYs with higher Si/Al ratios of 15 and 30 (i.e., Zeolyst CBV720 and CBV760, respectively) and detect UZM-35 only as a trace phase after 4 days of heating. To facilitate UZM-35 crystallization, therefore, we added a small amount (4 wt% relative to the amount of USY used as a Si source) of calcined UZM-35(C) as seed crystals to the synthesis mixture and carried out the synthesis for the same period of time. As shown in Table 1, we were then able to obtain pure UZM-35 in a highly reproducible manner.

Table 1 also lists the summary of the one-pot synthesis of Fe-UZM-35 performed in this study. The elemental analysis in Table 2 indicates that the Si/Al ratio (8) of UZM-35(IZC) from synthesis run 7 is slightly higher

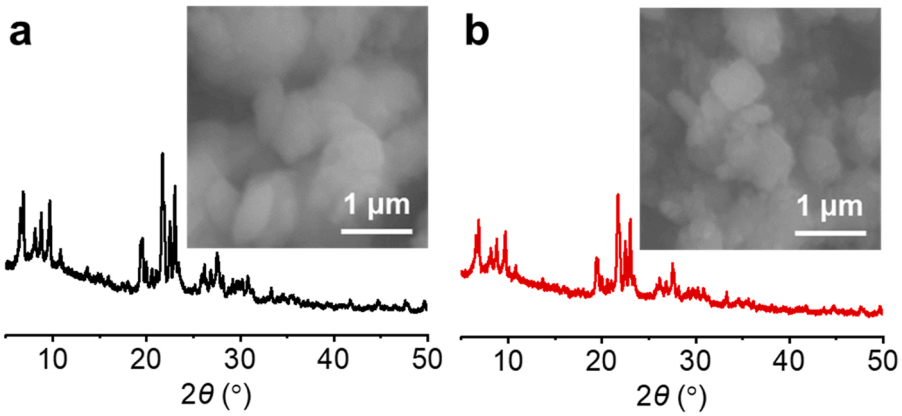

Fig. 2. PXRD patterns and SEM images of as-made (a) UZM-35(IZC) and (b) Fe-UZM-35(OP) obtained from synthesis runs 7 and 9 in Table 1, respectively.

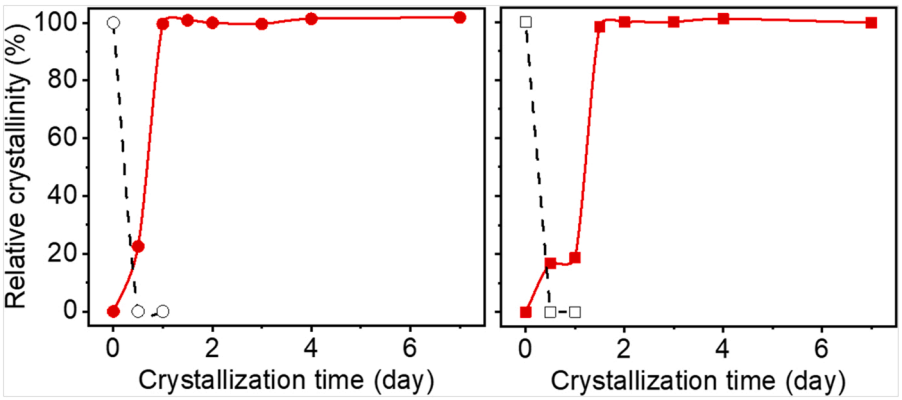

Fig. 3. Crystallinities of a series of solid products isolated as a function of time during the synthesis of UZM-35(IZC) (left) and Fe-UZM-35(OP) (right) using the same gels as those of synthesis runs 7 and 9 in Table 1 under static conditions at 170 °C, respectively. Open symbols indicate the crystallinity decrease of the CBV760 USY source.

than that (7) from synthesis run 5. Therefore, various amounts of ferric sulfate were added as an Fe source to the gel used to produce the former material and subject to crystallization at 170 °C, because the hydrothermal stability of metal-exchanged zeolites for NH_3-SCR becomes higher with increasing zeolite Si/Al ratio [2]. When the Fe/Al ratio in the synthesis mixture was 15 or lower, pure Fe-UZM-35 was obtained after 4 days of heating. However, we were not able to fully crystallize Fe-UZM-35 from the synthesis mixture with a higher Fe content (e.g., Fe/Al = 30). It is worth noting that while the use of cupric sulfate instead of ferric sulfate under the above synthesis conditions gave Cu-UZM-35, the Cu/Al ratio range (0−5) yielding its pure phase is significantly lower than the Fe/Al ratio range (0−15) for Fe-UZM-35 formation. As a spectator, therefore, the Fe^{2+} ion appears to disturb UZM-35 crystallization than the Cu^{2+} ion.

The PXRD patterns of as-made UZM-35(IZC) zeolites synthesized here reveal that they are highly crystalline (Fig. 2), as supported by the micropore volumes of their proton forms (Table 2). In particular, there are no reflections from other crystalline phases, which is also the case for as-made Fe-UZM-35(OP) and Cu-UZM-35(OP) zeolites with different Fe/Al (or Cu/Al) ratios (Supplementary Fig. S1). Thus, if any iron or copper oxide species were generated during the one-pot synthesis, their size may not be large enough to be detectable by PXRD. The ^{27}Al MAS NMR spectra of as-made UZM-35(IZC) and Fe-UZM-35(OP) are characterized by only one resonance around 55 ppm (Supplementary Fig. S2), typical of tetrahedral Al in the zeolite framework. Given that their Si/Al ratio (8) are considerably lower than the ratio (30) of the USY source, a major amount of silica from USY during IZC remains in solution, explaining the low product yield (ca. 25%) of IZC-synthesized UZM-35 and one-pot-synthesized Fe-UZM-35. We also note that as-made UZM-35 (IZC) and Fe-UZM-35(OP) show similar OSDA contents (Supplementary Fig. S3) and morphologies (Fig. 2) to each other, although their plate-like crystals are less faceted than UZM-35(C) crystals [21].

Fig. 3 shows the crystallization kinetics under static conditions at 170 °C of UZM-35(IZC) and Fe-UZM-35(OP) from gel compositions used for synthesis runs 7 and 9 in Table 1, respectively. It can be seen that their synthesis is almost complete after 1.0 and 1.5 days of heating, respectively. These crystallization times are quite shorter than the UZM-35(C) crystallization time (7 days), most likely because of the UZM-35 (C) seed crystals added. Notably, the retarding effect of Fe^{2+} spectator ions on UZM-35 formation is not strong. The fact that all characteristic X-ray peaks from USY entirely disappear within the first 12 h of the synthesis (Supplementary Fig. S4) suggests the dissolution of CBV760 USY crystals in the early stages, prior to UZM-35 formation.

3.2. NH_3-SCR

Fig. 4 shows the NO conversion as a function of reaction temperature over three pairs of Fe-UZM-35(C) and Fe-UZM-35(OP) catalysts with the same zeolite Si/Al ratio (9 or 8) but different Fe/Al ratios (0.13–0.38) in the fresh and 750 °C-aged forms under standard SCR conditions, with 10% H_2O present in the feed. All fresh Fe-UZM-35(C) catalysts exhibited quite similar SCR activities to one another in the reaction temperature region studied (150–600 °C), regardless of the Fe/Al ratio. The same trend could be observed for their 750 °C-aged form, although the low-temperature (<350 °C) NO conversion was rather lower than that of the corresponding fresh UZM-35(C) catalysts [21]. As shown in Fig. 4,

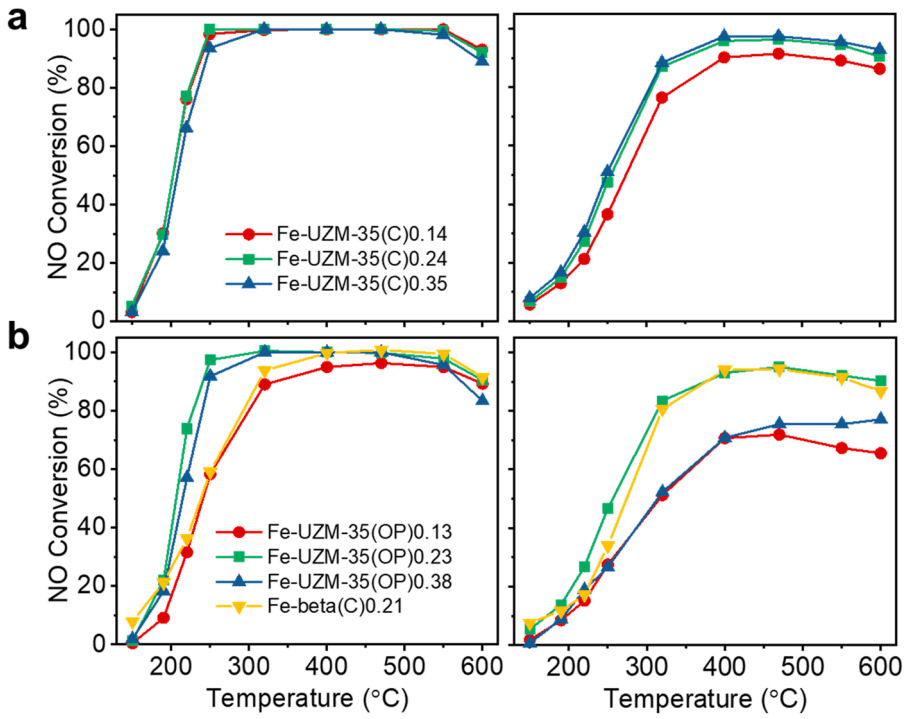

Fig. 4. NO conversion as a function of reaction temperature over the fresh (left) and 750 °C-aged (right) forms of (a) Fe-UZM-35(C) and (b) Fe-UZM-35(OP) with different Fe/Al ratios and Fe-beta(C)0.21. The feed contains 500 ppm NH_3, 500 ppm NO, 5% O_2 and 10% H_2O balanced with N_2 at 100,000 h^{-1} GHSV. Hydrothermal aging was carried out under flowing air containing 10% H_2O at 750 °C for 12 h.

however, there are notable differences in the NH_3-SCR activity of Fe-UZM-35(OP) catalysts, depending on the Fe/Al ratio. For example, the NO conversion over fresh catalysts at 250 °C was higher in the order Fe-UZM-35(OP)0.13 < Fe-UZM-35(OP)0.38 ≈ Fe-UZM-35(OP)0.23. In addition, the NO conversion over 750 °C-aged catalysts at the same reaction temperature increased in the order Fe-UZM-35(OP)0.38 ≈ Fe-UZM-35(OP)0.13 < Fe-UZM-35(OP)0.23. It is interesting to note that fresh Fe-UZM-35(OP)0.23 exhibits significantly higher in low-temperature NH_3-SCR activity than fresh Fe-beta(C)0.21, although the low-temperature activity becomes comparable after hydrothermal aging at 750 °C [11].

When differences in the framework Si/Al ratio of zeolite supports are not so large, in general, the standard SCR activity of Fe-exchanged zeolites are known to be less sensitive to the Fe loading level (or the Fe/Al ratio) than that of Cu-exchanged ones [28,29]. On the other hand, the conditions (170 ℃, autogenic pressure, and air atmosphere) during the one-pot synthesis of Fe-UZM-35 would be considerably different from those (80 ℃, atmospheric pressure, and N_2 atmosphere) during iron exchange in NH_4-UZM-35. It is then not difficult to expect that the state or intrazeolitic location of iron species in Fe-UZM-35(OP) could also be different from those in Fe-UZM-35(C). This may in our view be the major reason for the strong dependence of the SCR activity of Fe-UZM-35(OP) catalysts on their Fe/Al ratio. As shown in Fig. 4, however, the activity of Fe-UZM-35(OP)0.23 in both fresh and 750 °C-aged forms is essentially identical to that of Fe-UZM-35(C)0.24. The same result was also observed for the SCR activities of Cu-UZM-35(C)0.11 and Cu-UZM-35(OP)0.11 (Supplementary Fig. S5). Therefore, it is clear that Fe-UZM-35 with a high low-temperature activity can be conveniently and reproducibly one-pot synthesized, without careful iron exchange under inert N_2 atmosphere. We also note that the amount of N_2O formed during NH_3-SCR over Fe-UZM-35(OP) catalysts under the conditions employed here is negligible (Supplementary Fig. S6), like the case for Fe-UZM-35(C) [21].

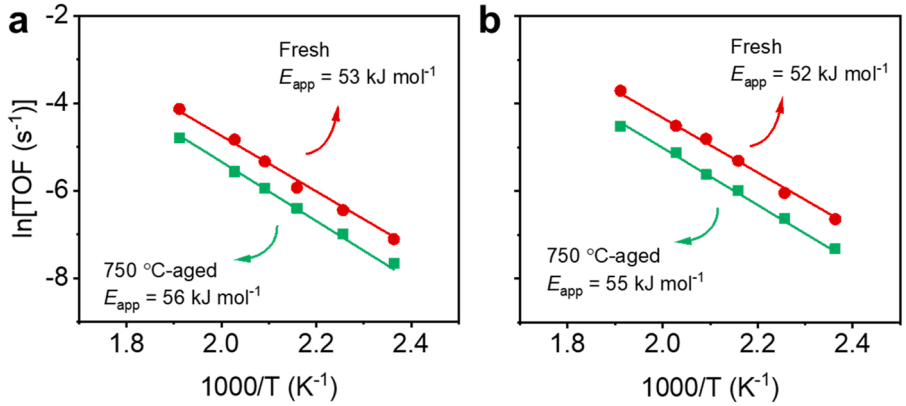

Fig. 5. Arrhenius plots for NH_3-SCR over the fresh and 750 °C-aged forms of (a) Fe-UZM-35(C)0.23 and (b) Fe-UZM-35(OP)0.24. Reaction conditions are the same as those in Fig. 4.

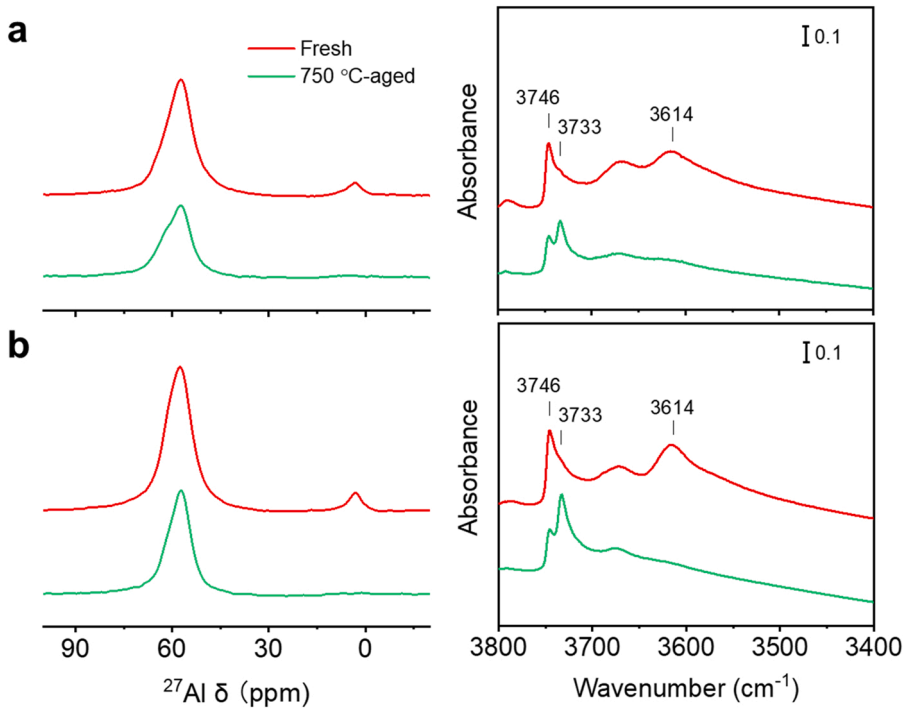

Fig. 6. ^{27}Al MAS NMR (left) and IR (right) spectra in the OH region of the fresh and 750 °C-aged forms of (a) Fe-UZM-35(C)0.23 and (b) Fe-UZM-35(OP)0.24.

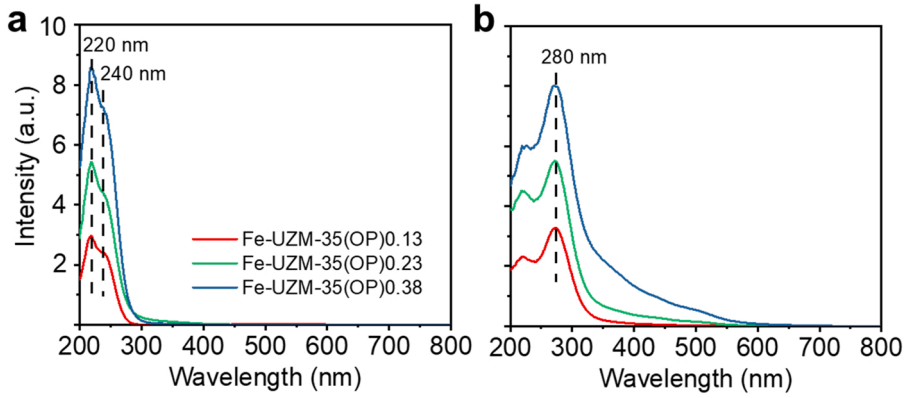

Fig. 7. UV-Vis spectra of the (a) as-made and (b) 550 °C-calcined forms of Fe-UZM-35(OP)0.13, Fe-UZM-35(OP)0.23, and Fe-UZM-35(OP)0.38.

3.3. Characterization

Fig. 5 shows the Arrheniuns plots of Fe-UZM-35(C)0.24 and Fe-UZM-35(OP)0.23 for standard NH_3-SCR. No noticeable differences (52–56 kJ mol^{-1}) in the E_{app} value were observed for their fresh form, but also their 750 °C-aged one. This does not allow the active sites in the former catalyst to be distinguished from those in the latter one, again showing the merit of the one-pot synthesis of Fe-UZM-35. The PXRD patterns of three 750 °C-aged Fe-UZM-35(OP) catalysts with Fe/Al = 0.13–0.38 gave reflections from the MSE structure only (Supplementary Fig. S1). It thus appears that the formation of large iron oxide particles on the external surface of the zeolite crystals during hydrothermal aging at 750 °C may not be significant. The ^{27}Al MAS NMR spectra of the fresh and 750 °C-aged forms of Fe-UZM-35(C)0.24 and Fe-UZM-35(OP)0.23 are compared in Fig. 6. An additional weak ^{27}Al signal around 0 ppm is observed for the fresh form of both catalysts. Moreover, the tetrahedral ^{27}Al signal resonance is considerably weaker for their 750 °C-aged form, because of severe dealumination during hydrothermal aging. This can be further supported by their IR spectra in the OH region. As shown in Fig. 6, the OH band appearing at 3614 cm^{-1} due to Si-OH-Al Brønsted acid sites [11] is hardly observable for 750 °C-aged Fe-UZM-35(C)0.24 and Fe-UZM-35(OP)0.23 both, which matches well with a notable intensity increase of the IR band at 3733 cm^{-1}, assignable to internal Si-OH groups [30,31]. It is also remarkable that the acidic properties of the fresh and 750 °C-aged forms of Fe-UZM-35(OP)0.23 have a strong resemblance to those of the corresponding forms of Fe-UZM-35(C)0.24, respectively, because the NH_3 TPD profiles of these two pair of Fe-UZM-35 catalysts are characterized by similar line shapes and areas (Supplementary Fig. S7).

Fig. 7 shows the UV-Vis spectra of the as-made and 550 °C-calcined forms of three Fe-UZM-35(OP) zeolites with different Fe/Al ratios (0.13–0.38) in the hydrated state. The spectra of all as-made zeolites have almost the same line shape so that two $Fe^{3+} \leftarrow O$ charge-transfer (CT) bands around 220 and 240 nm, attributable to the isolated framework Fe^{3+} ions [32], can be resolved, with nearly constant relative intensities. In fact, we cannot exclude the possibility that partial Fe substitution has occurred during UZM-35(OP) synthesis, because no specific iron chelating agents were intentionally added to the synthesis mixture. As shown in Fig. 7, on the other hand, calcination of as-made Fe-UZM-35(OP) zeolites at 550 °C results in the appearance of a new

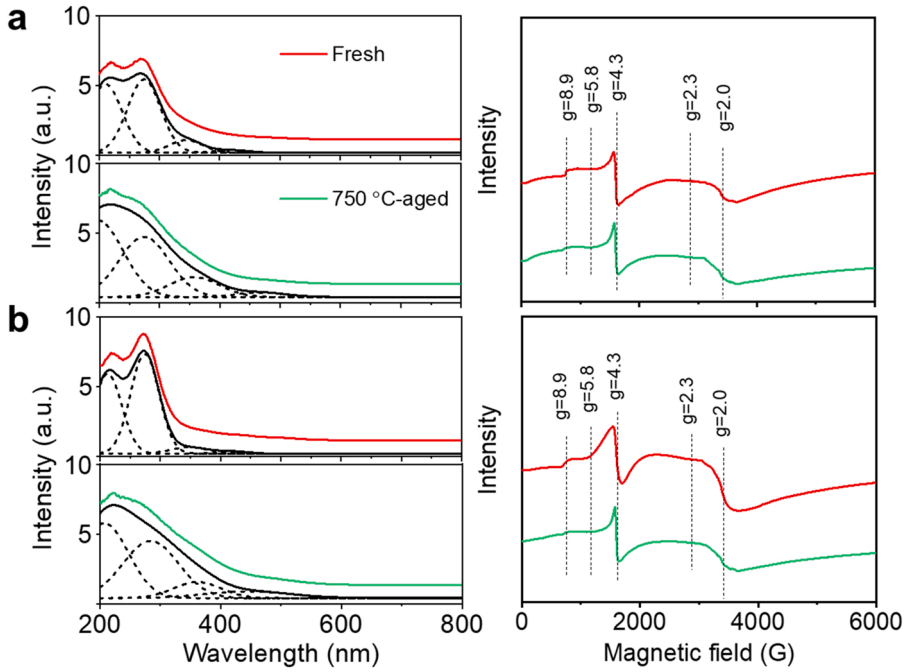

Fig. 8. UV-Vis (left) and EPR (right) spectra of the fresh and 750 °C-aged forms of (a) Fe-UZM-35(C)0.23 and (b) Fe-UZM-35(OP)0.24. The EPR spectra were collected at − 148 ℃.

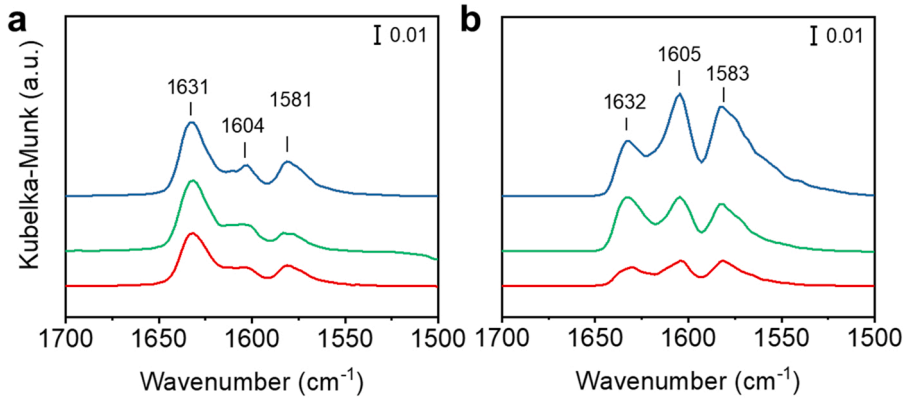

Fig. 9. DRIFT spectra of NO adsorbed on fresh (a) Fe-UZM-35(C)0.14, Fe-UZM-35(C)0.24, and Fe-UZM-35(C)0.35 (bottom to top) and (b) Fe-UZM-35(OP)0.13, Fe-UZM-35(OP)0.23, and Fe-UZM-35(OP)0.38 (bottom to top). All the spectra were recorded at 150 °C after exposure to the feed gas containing 500 ppm NO and 5% O_2 in He flow for 1 h followed by purging in a He flow at the same temperature for another 0.5 h.

strong band around 280 nm. This implies that well-dispersed extra-framework Fe^{3+} ions in octahedral coordination may be one of the major iron species in calcined Fe-UZM-35(OP) zeolites [18].

Fig. 8 shows the UV-Vis spectra of the fresh and 750 °C-aged forms of Fe-UZM-35(C)0.24 and Fe-UZM-35(OP)0.23 in the hydrated state. The spectra of both fresh catalysts exhibit two CT bands around 220 and 280 nm, together with two weaker CT bands around 350 and 450 nm that can be attributed to small Fe_xO_y clusters and larger Fe_2O_3 particles, respectively [33,34]. While the band around 280 nm becomes weaker after hydrothermal aging at 750 °C, the opposite holds for the two bands around 220 and 280 nm. Deconvolution of the UV-Vis spectra in Fig. 8 reveals that the relative intensity distribution of these four CT bands is nearly the same for the two pairs of Fe-UZM-35 catalysts (Supplementary Table S1). Also, hydrothermal aging at 750 °C led to no decrease in relative intensity for the band around 220 nm ascribed to tetrahedral Fe^{3+} ions. The same result was found in the UV-Vis spectra (not shown) of two pairs of Fe-UZM-35(C) and Fe-UZM-35(OP) zeolites with lower (ca. 0.13) and higher (ca. 0.36) Fe/Al ratios. Therefore, the octahedral extra-framework Fe^{3+} ions appear to be more responsible for the high low-temperature (<350 ℃) SCR activity of fresh Fe-UZM-35, because water is among the key components in vehicle exhaust. The X-band EPR spectra at − 148 ℃ of the above four catalysts are also compared in Fig. 8. No noticeable changes in the EPR line shape by hydrothermal aging were observed, except some intensity decrease of the two low-field signals at *g* values of 8.9 and 5.8, probably owing to the partial transformation of isolated Fe^{3+} species to iron oxide species [35,36].

Fig. 9 shows the DRIFT spectra of adsorbed NO on three pairs of fresh Fe-UZM-35(C) and Fe-UZM-35(OP) catalysts with different Fe/Al ratios. All the spectra are characterized by three bands at 1632, 1605, and 1583 cm^{-1}. The first band at 1632 cm^{-1} is assigned to Fe^{3+} mononitrosyl species, whereas the other two bands at 1605 and 1583 cm^{-1} reflect the formation of Fe^{3+} nitrate species, respectively [37–39]. No dependence of the relative intensity on Fe/Al ratio was observed for these three bands from fresh Fe-UZM-35(C) catalysts. As shown in Fig. 9, however, this is not the case for Fe-UZM-35(OP) ones. For example, the two bands at 1605 and 1583 cm^{-1} become stronger with increasing

Fe/Al ratio from 0.13 to 0.38. Also, the relative intensity of the band at 1632 cm^{-1} is significantly weaker from Fe-UZM-35(OP)0.13 than from Fe-UZM-35(C)0.14, despite essentially the same Fe/Al ratio (ca. 0.13). Recall that the low-temperature activity of the former catalyst is considerably poorer than that of the latter one (Fig. 4). We speculate that this can be attributed to differences in the intrazeolitic location of their isolated Fe^{3+} ions, which deserves further study.

Finally, we have also carried out UV–vis and Cu K-edge XANES measurements on the fresh and 750 °C-aged forms of Cu-UZM-35(C) 0.10 and Cu-UZM-35(OP)0.11 catalysts. No noticeable differences in the type and distribution of various copper species in their respective Cu-UZM-35 catalysts were found (Supplementary Table S2 and Figs. S8 and S9), in line with their SCR activities (Supplementary Fig. S5).

4. Conclusions

In summary, we have synthesized the large-pore zeolite UZM-35 by combining the IZC route with the seeding method, using USY zeolites as both Al and Si-sources in the presence of DMDPA as an OSDA. We were also successful in the one-pot-synthesis of Fe-UZM-35 which is much more convenient and reproducible than the post-synthetic preparation of iron-exchanged UZM-35, because there is no need for careful iron exchange under N_2 atmosphere and repeated calcination steps. This route also allows Fe-UZM-35 crystallization to be complete within 1.5 days, which is considerably shorter than the crystallization time (7 days) of conventional UZM-35. The NH_3-SCR activities of one-pot-synthesized and post-synthetically exchanged Fe-UZM-35 zeolites with similar Fe/Al ratios (ca. 0.23) were found to be essentially identical to each other in the reaction temperature range studied, regardless of hydrothermal aging at 750 ℃. The overall characterization results show no notable differences in the nature of their iron active sites. However, the intrazeolitic location of isolated Fe^{3+} ions, known as active sites for low-temperature NH_3-SCR, could be different because of notable differences in the temperature, pressure, and atmosphere of the one-pot Fe-UZM-35 synthesis compared to iron exchange in NH_4-UZM-35. We expect that this study will provide useful insight into the facile synthesis of metal-loaded zeolites with interesting NH_3-SCR performance but poor synthesis reproducibility.

CRediT authorship contribution statement

Xuechao Tan: Conceptualization, Methodology, Investigation, Writing – original draft. **Shoute Zhang:** Conceptualization, Methodology, Investigation, Writing – original draft. **Suk Bong Hong:** Conceptualization, Supervision, Writing – review & editing, Project administration, Funding acquisition.

Declaration of Competing Interest

The authors declare that they have no known competing financial interests or personal relationships that could have appeared to influence the work reported in this paper.

Data Availability

Data will be made available on request.

Acknowledgements

This work was supported by the National Creative Research Initiative Program (2021R1A3A3088711) through the National Research Foundation of Korea. We thank K. Lee (POSTECH) for helpful discussion. We also thank PAL for beam time at 8 C (K.-S. Lee). PAL is supported by MSIP and POSTECH.

Appendix A. Supporting information

Supplementary data associated with this article can be found in the online version at doi:10.1016/j.apcatb.2023.122552.

References

[1] A.S.K. Raju, B.R. Wallerstein, K.C. Johnson, Achieving NO_x and greenhouse gas emissions goals in California's Heavy-Duty transportation sector, Transp. Res. D. 97 (2021), 102881.
[2] A.M. Beale, F. Gao, I. Lezcano-Gonzalez, C.H.F. Peden, J. Szanyi, Recent advances in automotive catalysis for NO_x emission control by small-pore microporous materials, Chem. Soc. Rev. 44 (2015) 7371–7405.
[3] L. Han, S. Cai, M. Gao, J. Hasegawa, P. Wang, J. Zhang, L. Shi, D. Zhang, Selective catalytic reduction of NO_x with NH_3 by using novel catalysts: State of the art and future prospects, Chem. Rev. 119 (2019) 10916–10976.
[4] J. Li, X. Meng, F.-S. Xiao, Zeolites for control of NO_x emissions: opportunities and challenges, Chem. Catal. 2 (2022) 253–261.
[5] I. Bull, W.-M. Xue, P. Bruk, R.S. Boorse, W.M. Jaglowski, G.S. Koermer, A. Moini, J. A. Patchett, J.C. Dettling, M.T. Caudle, Copper CHA zeolite catalysts, US Patent 7,601,662B2 (2009).
[6] M. Moliner, C. Franch, E. Palomares, M. Grill, A. Corma, Cu–SSZ-39, an active and hydrothermally stable catalyst for the selective catalytic reduction of NO_x, Chem. Commun. 48 (2012) 8264–8266.
[7] A.R. Ravishankara, J.S. Daniel, R.W. Portmann, Nitrous Oxide (N_2O): The dominant ozone-depleting substance emitted in the 21st century, Science 326 (2009) 123–125.
[8] M. Colombo, I. Nova, E. Tronconi, A comparative study of the NH_3-SCR reactions over a Cu-zeolite and a Fe-zeolite catalyst, Catal. Today 151 (2010) 223–230.
[9] X. Feng, W.K. Hall, FeZSM-5: A durable SCR catalyst for NO_x removal from combustion streams, J. Catal. 166 (1997) 368–376.
[10] T. Ryu, Y. Kang, I.-S. Nam, S.B. Hong, Iron-exchanged high-silica LTA zeolites as hydrothermally stable NH_3-SCR catalysts, React. Chem. Eng. 4 (2019) 1050–1058.
[11] T. Ryu, S.B. Hong, Iron-exchanged UZM-35: An active NH_3-SCR catalyst at low temperatures, Appl. Catal. B 266 (2020), 118622.
[12] F. Gao, M. Kollára, R.K. Kukkadapu, N.M. Washton, Y. Wang, J. Szanyi, C.H. F. Peden, Fe/SSZ-13 as an NH_3-SCR catalyst: a reaction kinetics and FTIR/Mössbauer spectroscopic study, Appl. Catal. B 164 (2015) 407–419.
[13] L. Ren, L. Zhu, C. Yang, Y. Chen, Q. Sun, H. Zhang, C. Li, F. Nawaz, X. Meng, F.-S. Xiao, Designed copper-amine complex as an efficient template for one-pot synthesis of Cu-SSZ-13 zeolite with excellent activity for selective catalytic reduction of NO_x by NH_3, Chem. Commun. 47 (2011) 9789–9791.
[14] F. Gao, E.D. Walter, N.M. Washton, J. Szanyi, C.H.F. Peden, Synthesis and evaluation of Cu/SAPO-34 catalysts for NH_3-SCR 2: Solid-state ion exchange and one-pot synthesis, Appl. Catal. B 162 (2015) 501–514.
[15] L. Ren, Q. Wu, C. Yang, L. Zhu, C. Li, P. Zhang, H. Zhang, X. Meng, F.-S. Xiao, Solvent-free synthesis of zeolites from solid raw materials, J. Am. Chem. Soc. 134 (2012) 15173–15176.
[16] S. Andonova, S. Tamm, L. Olsson, C.N. Montreuil, C.K.Lambert. Fe-SAPO-34 catalyst for use in NO_x reduction and method of making. US Patent 20150231617 (2015).
[17] E. Yuan, G. Wu, W. Dai, N. Guan, L. Li, One-pot construction of Fe/ZSM-5 zeolites for the selective catalytic reduction of nitrogen oxides by ammonia, Catal. Sci. Technol. 7 (2017) 3036.
[18] N. Martín, P.N.R. Vennestrøm, J.R. Thøgersen, M. Moliner, A. Corma, Fe-containing zeolites for NH_3-SCR of NO_x: Effect of structure, synthesis procedure, and chemical composition on catalytic performance and stability, Chem. Eur. J. 23 (2017) 13404–13414.
[19] N. Martín, P.N.R. Vennestrøm, J.R. Thøgersen, M. Moliner, A. Corma, Iron-containing SSZ-39 (AEI) Zeolite: an active and stable high-temperature NH_3-SCR catalyst, ChemCatChem 9 (2017) 1754–1757.
[20] M.L. Bols, J. Devos, H.M. Rhoda, D. Plessers, E.I. Solomon, R.A. Schoonheydt, B. F. Sels, M. Dusselier, Selective formation of α-Fe(II) sites on Fe-zeolites through one-pot synthesis, J. Am. Chem. Soc. 143 (2021) 116243–116255.
[21] J.H. Lee, Y.J. Kim, T. Ryu, P.S. Kim, C.H. Kim, S.B. Hong, Synthesis of zeolite UZM-35 and catalytic properties of copper-exchanged UZM-35 for ammonia selective catalytic reduction, Appl. Catal. B 200 (2017) 428–438.
[22] S.I. Zones, R.A. Van Nordstrand, Novel zeolite transformations: the template-mediated conversion of cubic P zeolite to SSZ-13, Zeolites 8 (1988) 166–174.
[23] S.I. Zones, R.A. Van Nordstrand, Further studies on the conversion of cubic P zeolite to high silica organozeolites, Zeolites 8 (1988) 409–415.
[24] S.I. Zones, Conversion of faujasites to high-silica chabazite SSZ-13 in the presence of *N,N,N*-trimethyl-1-adamantammonium iodide, J. Chem. Soc., Faraday Trans. 87 (1991) 3709–3716.
[25] M. Dusselier, M.E. Davis, Small-pore zeolites: synthesis and catalysis, Chem. Rev. 118 (2018) 5265–5329.
[26] C. Baerlocher, L.B. McCusker, Database of Zeolite Structures, http://www.iza-structure.org/databases/ (accessed 25.01.22).
[27] K. Lee, S.H. Cha, S.B. Hong, MSE-Type zeolites: a promising catalyst for the conversion of ethene to propene, ACS Catal. 6 (2016) 3870–3874.
[28] F. Gao, E.D. Walter, M. Kollar, Y. Wang, J. Szanyi, C.H.F. Peden, Understanding ammonia selective catalytic reduction kinetics over Cu/SSZ-13 from motion of the Cu ions, J. Catal. 319 (2014) 1–14.

[29] P. Chen, R. Moos, U. Simon, Metal loading affects the proton transport properties and the reaction monitoring performance of Fe-ZSM-5 and Cu-ZSM-5 in NH_3-SCR, J. Phys. Chem. C. 120 (2016) 25361–25370.
[30] A. Zecchina, S. Bordiga, G. Spoto, L. Marchese, G. Petrini, G. Leofanti, M. Padovan, Silicalite characterization. 2. IR spectroscopy of the interaction of carbon monoxide with internal and external hydroxyl groups, J. Phys. Chem. 96 (1992) 4991–4997.
[31] C. Yang, Q. Xu, States of aluminum in zeolite β and influence of acidic or basic medium, Zeolites 19 (1997) 404–410.
[32] S. Bordiga, R. Buzzoni, F. Geobaldo, C. Lamberti, E. Giamello, A. Zecchina, G. Leofanti, G. Petrini, G. Tozzolo, G. Vlaic, Structure and reactivity of framework and extraframework iron in Fe-silicalite as investigated by spectroscopic and physicochemical methods, J. Catal. 158 (1996) 486–501.
[33] R.P. Vélez, I. Ellmers, H. Huang, U. Bentrup, V. Schünemann, W. Grünert, A. Brückner, Identifying active sites for fast NH_3-SCR of NO/NO_2 mixtures over Fe-ZSM-5 by operando EPR and UV–vis spectroscopy, J. Catal. 316 (2014) 103–111.
[34] P. Marturano, L. Drozdová, G.D. Pirngruber, A. Kogelbauer, R. Prins, The mechanism of formation of the Fe species in Fe/ZSM-5 prepared by CVD, Phys. Chem. Chem. Phys. 3 (2001) 5585–5595.
[35] M.S. Kumar, M. Schwidder, W. Grünert, A. Brückner, On the nature of different iron sites and their catalytic role in Fe-ZSM-5 $DeNO_x$ catalysts: new insights by a combined EPR and UV/VIS spectroscopic approach, J. Catal. 227 (2004) 384–397.
[36] L. Kovarik, N.M. Washton, R. Kukkadapu, A. Devaraj, A. Wang, Y. Wang, J. Szanyi, C.H.F. Peden, F. Gao, Transformation of active sites in Fe/SSZ-13 SCR catalysts during hydrothermal aging: a spectroscopic, microscopic, and kinetics study, ACS Catal. 7 (2017) 2458–2470.
[37] H.-Y. Chen, T. Voskoboinikov, W.M.H. Sachtler, Reduction of NO_x over Fe/ZSM-5 catalysts: adsorption complexes and their reactivity toward hydrocarbons, J. Catal. 180 (1998) 171–183.
[38] G. Mul, J. Pérez-Ramírez, F. Kapteijn, A. Moulijn, NO adsorption on ex-framework [Fe,X]MFI catalysts: novel IR bands and evaluation of assignments, Catal. Lett. 80 (2002) 129–138.
[39] L.J. Lobree, I.-C. Hwang, J.A. Reimer, A.T. Bell, An in situ infrared study of NO reduction by C_3H_8 over Fe-ZSM-5, Catal. Lett. 63 (1999) 233–240.